metals

MDPI

Article

Effect of CaO-MgO-FeO-SiO_2-xNa_2O Slag System on Converter Dephosphorization

Bin Geng [1], Dongping Zhan [1,*], Zhouhua Jiang [1] and Yongkun Yang [2]

[1] School of Metallurgy, Northeastern University, Shenyang 110819, China; 2071501@stu.neu.edu.cn (B.G.)
[2] School of Metallurgical Engineering, Xi'an University of Architecture and Technology, Xi'an 710055, China
* Correspondence: zhandp@smm.neu.edu.cn

Abstract: Na_2O is an alkaline oxide, which can significantly improve the dephosphorization ability of converter slag. The effect of Na_2O on the dephosphorization of converter slag was analyzed with a high-temperature dephosphorization experiment in a $MoSi_2$ resistance furnace. We found that the dephosphorization rate increased with the increase of (Na_2O) in the dephosphorization slag. The elements of Ca, Si, O, and P in the dephosphorization slag are distributed in the same area, mainly in the form of phosphate minerals, such as $Ca_2SiO_4 \cdot 0.05Ca_3(PO_4)_2$ and $6Ca_2SiO_4 \cdot Ca_3(PO_4)_2$. After adding Na_2O, part of the Na will replace the Ca in the phosphorus-containing phase to form $Ca_2SiO_4 \cdot Ca_2Na_2(PO_4)_2$. The industrial test showed that the average dephosphorization rate in the early stage of the test heats with the CaO-MgO-FeO-SiO_2-0.5%Na_2O slag system could reach 62.39%, which was 19.62% higher than that of the conventional heats. The average basicity of the final slag was 0.19% lower than that of the conventional heats, while $w(P_2O_5)$ increased by 0.36%, and T.Fe decreased by 0.69%. The average consumption of the slagging materials was 35.93 kg/t, which was 7.24 kg/t less than that of the conventional heats. Through thermodynamic calculation, we found that with the increase of (Na_2O), the phosphorus distribution ratio between slag and steel increased significantly, the area of the liquid phase zone of the slag system increased continuously, and the viscosity decreased continuously.

Keywords: CaO-MgO-FeO-SiO_2-xNa_2O slag system; converter dephosphorization; thermodynamic calculation; slag properties

check for updates

Citation: Geng, B.; Zhan, D.; Jiang, Z.; Yang, Y. Effect of CaO-MgO-FeO-SiO_2-xNa_2O Slag System on Converter Dephosphorization. *Metals* **2023**, *13*, 844. https://doi.org/10.3390/met13050844

Academic Editor: Mark E. Schlesinger

Received: 4 April 2023
Revised: 19 April 2023
Accepted: 23 April 2023
Published: 25 April 2023

Copyright: © 2023 by the authors. Licensee MDPI, Basel, Switzerland. This article is an open access article distributed under the terms and conditions of the Creative Commons Attribution (CC BY) license (https://creativecommons.org/licenses/by/4.0/).

1. Introduction

For most steel, phosphorus is a harmful element, and its segregation in steel will cause uneven structure, reduce the plasticity and toughness of steel, cause 'cold brittleness', and seriously affect its service performance [1]. Therefore, in order to meet the market demand for low-phosphorus steel, various converter dephosphorization processes have been developed by major steel mills, for example, the MURC (Multi-Refining Converter) of Nippon Steel [2], the SGRS (Slag Generation Reduced Steelmaking) of Shougang [3,4], and the BRP (BOF Refining Process) of Baosteel [5]. These processes mainly rely on the converter double slag method or the duplex method to achieve dephosphorization. Converter slag is mainly produced by the oxidation of silicon, phosphorus, iron, manganese, and other elements in molten iron and the addition of lime, dolomite, and other slagging materials. In addition, there are some other ways of formation, such as the blast furnace slag brought into the converter and the eroded converter lining [6]. In 2021, Chinese crude steel production reached 1.03 billion tons, and the byproduct converter slag in the smelting process also increases year by year. At present, about 1 billion tons of slag are stored in China, occupying a large amount of land and polluting the environment.

Reducing the amount of converter slag has important economic and ecological benefits. In this regard, metallurgical scholars are committed to developing new dephosphorization slag [7–15] to enhance the dephosphorization efficiency. Pak J J [8,9] studied the effect of

Na_2O on the dephosphorization of CaO-based steelmaking slag. Adding Na_2O to CaO-SiO_2 slag will increase the phosphorus distribution ratio. At 1873 K, adding 6% Na_2O to CaO-saturated CaO-FeO-SiO_2 slag can increase the L_P by 5 times. For slag with high binary basicity due to the high activity of Na_2O, even if $w(Na_2O)$ is low, the effect of Na_2O on L_P is also significant. Guangqiang Li [10] studied the effect of Na_2O and Al_2O_3 on the dephosphorization of high basicity CaO-FeO-SiO_2 slag under the MgO saturation condition. They found that the addition of Na_2O in MgO-saturated CaO-FeO-SiO_2 slag can increase the phosphate capacity of slag. When $w(Na_2O)$ increased from 0 to 1.75%, the phosphate capacity increased from $10^{18.37}$ to 10^{19}. Jiang Diao [11] added a small amount of Na_2O and Al_2O_3 to fluorine-free CaO-FeO-SiO_2 slag to reduce the melting point and promote the dephosphorization reaction. When $w(Na_2O)$ and $w(Al_2O_3)$ in the dephosphorization slag reached 0.7~3.1% and 2.5~7.9%, respectively, the dephosphorization rate could reach 81.4~90.7%. Taposhe G.I.A. [16] used CaO-Al_2O_3-SiO_2-Na_2O slag to remove phosphorus from Si-Fe alloy and found that the presence of Na_2O in the slag increased the L_P. Fengshan Li [17,18] found that with the increasing of Na_2O, the phosphate capacity increased linearly, which showed that Na_2O can significantly affect the dephosphorization capacity of slag. Xianpeng Li [19] determined the phosphorus distribution ratio between CaO-FeO-SiO_2-Al_2O_3/Na_2O/TiO_2 slag and molten iron, and found that L_P increased rapidly with the increasing of $w(Na_2O)$ in slag. When the $w(Na_2O)$ in slag increased by 6.94%, L_P increased by 5.4 times, which indicated that Na_2O could significantly improve the dephosphorization ability of slag. Zhiqiang Zhou [20] studied the effect of adding Na_2O to the alkaline slag in the dephosphorization of silicon–manganese alloy at 1673 K. They found that adding a small amount of Na_2O to the dephosphorization slag could increase the phosphorus distribution ratio by 0.6%, and the corresponding dephosphorization rate increased by about 10%. Xinyu Xuan [21] studied the dephosphorization effect of CaO-SiO_2-FeO-Na_2O-Al_2O_3 slag on medium- and high-phosphorus molten iron. They found that when the dephosphorization slag contained both Al_2O_3 and Na_2O, the dephosphorization effect was better than that of Al_2O_3 or Na_2O alone. When the $w(Al_2O_3)$ in the dephosphorization slag was 4% and the $w(Na_2O)$ was 2%, the dephosphorization rate could reach 95.66%. In addition, some scholars [22–24] explored the effect of Na_2CO_3 on dephosphorization and found that it has a good dephosphorization effect and can be used as a dephosphorization agent. Ito K [25] found that the phosphate capacity of industrial waste residue treated with soda ash is very large, up to 10^{31}. Marukawa K [26] studied the treatment effect of sodium carbonate on molten iron and found that dephosphorization and desulfurization were carried out simultaneously. The addition of Na_2CO_3 reduced the melting point of CaO-based slag and improved the fluidity of slag.

In summary, Na_2O can effectively increase the phosphorus distribution ratio and improve the dephosphorization effect. In this paper, the effects of Na_2O additions on the mineral phase structure of slag were investigated through laboratory experiments. On this basis, industrial tests were carried out in a 130 t converter. A CaO-MgO-FeO-SiO_2-xNa_2O slag system was added in the early stage of smelting, and the appropriate slag addition system was matched to achieve the purpose of rapid slag melting and enhanced early dephosphorization. At the same time, the effects of Na_2O on the phosphorus distribution ratio between slag and steel, and the melting point and viscosity of the slag system were analyzed by thermodynamic calculation, which provided a basic theoretical reference for optimizing slag composition.

2. Experimental Method

2.1. Laboratory Experiment Scheme

2.1.1. High Temperature Dephosphorization Experimental Scheme

The iron sample used in the experiment was obtained by adding ferrophosphorus after the melting of pig iron. The composition of the pig iron was [C] = 3.31%, [Si] = 0.27%, [Mn] = 0.13%, and [P] = 0.08%, and the mass fraction of phosphorus in the ferrophosphorus

was 27.1%. The dephosphorization slag was obtained by pure chemical reagents, such as CaO and SiO_2, in a certain ratio (Na_2O is replaced by Na_2CO_3).

Before the high temperature dephosphorization experiment, the initial molten iron was prepared by the pre-melting of pig iron and ferrophosphorus; the compositions are shown in Table 1. Then, the high-temperature dephosphorization experiment was carried out in the $MoSi_2$ resistance furnace; the experimental device is shown in Figure 1. The 400 g molten iron sample was put into the magnesium oxide crucible (φ60 mm × 72 mm) of the outer-sleeve graphite crucible (φ70 mm × 100 mm) and put into the furnace. The sample was melted at 1653 K in an argon atmosphere, then 60 g of dephosphorization slag containing different amounts of Na_2CO_3 (the compositions are shown in Table 2) was added, followed by appropriate stirring to promote melting. After 30 min of reaction, the dephosphorization slag sample was taken with a molybdenum rod, and the molten iron sample was extracted with a quartz tube.

Table 1. Initial chemical compositions of molten iron (mass fraction, %).

C	Si	Mn	P	S
3.08	0.03	0.08	0.135	0.034

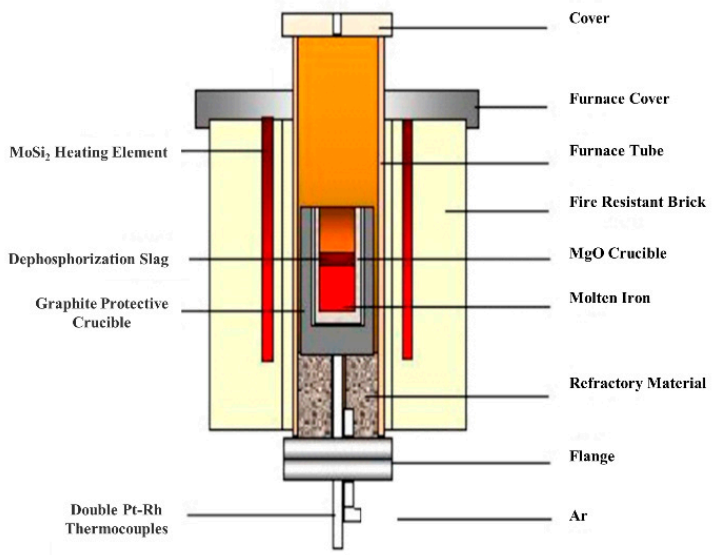


Figure 1. Schematic diagram of $MoSi_2$ resistance furnace.

Table 2. Compositions of dephosphorization slag (mass fraction, %).

Heats	Compositions						R
	CaO	Fe_2O_3	MgO	MnO	SiO_2	Na_2CO_3	
1	31.6	33.3	9	5	21.1	0	1.50
2	29.6	33.3	9	5	19.7	3.42	1.50
3	27.6	33.3	9	5	18.4	6.84	1.50
4	25.6	33.3	9	5	17.1	10.26	1.50

2.1.2. Melting Point Testing Scheme

In order to explore the effect of Na_2O on the melting point of the slag system, the melting point of the CaO-MgO-FeO-SiO_2-$x$$Na_2O$ slag system was tested with a slag melting characteristic tester. The hemispherical point temperature of the sample was defined as its melting temperature. Before the test, the samples were uniformly ground in agate mortar and mixed with anhydrous ethanol to make a 3 mm × 3 mm cylindrical sample. Each sample was heated at the same rate and tested 3 times to obtain the average.

2.1.3. Viscosity Calculation Method

Using FactSage8.1 to calculate the viscosity of the slag, we first opened the 'Viscosity' module. Then, we selected the component and entered its mass fraction (g) and input temperature (K), selected the viscosity unit (Pa·s), selected the 'Melts' melt database, and clicked the 'Calculate' button to calculate the relevant values.

2.2. Industrial Program

In order to improve the dephosphorization effect, the production process of a 130 t converter in a steel plant was improved, and the industrial test was carried out using CaO-MgO-FeO-SiO_2-$x$$Na_2O$ slag. The single-slag smelting process mode was adopted. After the blowing was stable, lime, magnesium oxide ball, and sodium-containing slag were added with the appropriate slagging method. Among them, lime was added in 6~7 batches, the magnesium oxide ball was added in 2 batches, and the sodium-containing slagging material was added in 2~3 batches. Due to the erosion effect of excessive alkaline oxide on the furnace lining, the $w(Na_2O)$ in the slag was controlled at about 0.5% in the early stage of the test heats to improve the dephosphorization effect. In the later stage of smelting, the basicity of the final slag should be controlled at 2.0~2.5. In the production process, the molten iron samples were taken by sublance at the 6 min blowing and the blowing end point, respectively, to compare the dephosphorization effect of each stage. The slag samples at the end of blowing were analyzed and compared.

2.3. Analysis Method

2.3.1. Analysis Method of Molten Iron Sample

The molten iron sample was polished with 600 mesh sandpaper to remove the surface oxide, and then the debris sample was obtained with a multifunctional drilling machine. Next, the mass fractions of carbon and sulfur were detected with an infrared carbon and sulfur analyzer (instrument model LECO-CS230), and the mass fractions of silicon, manganese, and phosphorus were detected with an inductively coupled plasma emission spectrometer (ICP, instrument model PE-Avio500).

2.3.2. Analysis Method of Slag Sample

The dephosphorization slag was ground into powder with a crusher and then screened with 200-mesh sieves to obtain a slag sample with a particle size meeting the detection standard. The composition of the slag sample was detected with an X-ray fluorescence spectrometer (XRF, ZSXPrimus II), and the Na_2O in the slag sample was detected by ICP. An X-ray diffractometer (XRD, Uitima IV) was used to detect and analyze the phase of the slag sample. The diffractometer used a copper target with a scanning range of 15–80° and a scanning speed of 10°/min. The morphology of the dephosphorization slag was observed with a tungsten filament scanning electron microscope (SEM, ZEISS EVO18), and the corresponding regions and locations were selected for energy dispersive spectroscopy (EDS) component surface analysis and point analysis.

3. Experimental Results

3.1. Laboratory Dephosphorization Experimental Results

The test results of the dephosphorization experiment are shown in Table 3, and the test results of the dephosphorization slag compositions are shown in Table 4. With the increasing of the $w(Na_2O)$ in the slag, the dephosphorization rate and phosphorus distribution ratio increased. After adding Na_2O with a mass fraction of about 1% to the slag, the dephosphorization rate reached 76.30%, and the phosphorus distribution ratio reached 5.24, which are 4.45% and 0.19% higher, respectively, than the heat without adding Na_2O, indicating that adding a small amount of Na_2O can improve the dephosphorization ability of the slag.

Table 3. Experimental dephosphorization results.

Heats	Compositions/%					Dephosphorization Rate/%	lgL_P/%
	C	Si	Mn	P	S		
No. 1	2.80	0.02	0.04	0.038	0.030	71.85	5.05
No. 2	2.67	0.01	0.05	0.032	0.030	76.30	5.24
No. 3	2.20	0.02	0.05	0.030	0.030	77.78	5.31
No. 4	1.80	0.02	0.04	0.029	0.032	78.52	5.36

Note: The L_P calculation formula is $L_P = \frac{(\%P_2O_5)_{slag}}{[\%P]^2_{molten\ iron}}$.

Table 4. Compositions of dephosphorization slag (mass fraction, %).

Heats	CaO	T.Fe	MgO	MnO	SiO_2	Na_2O	P_2O_5	R
No. 1	34.76	19.42	7.18	4.34	23.24	0.00	1.63	1.50
No. 2	33.56	17.41	8.74	3.44	22.67	0.94	1.76	1.48
No. 3	37.83	14.13	9.28	3.50	26.32	2.42	1.83	1.40
No. 4	36.31	16.02	10.05	3.60	24.32	2.98	1.92	1.49

Figure 2 shows the XRD patterns of the dephosphorization slag samples. Figure 2a indicates that the phosphorus element mainly exists in the form of phosphate phases, such as $Ca_2SiO_4{\cdot}0.05Ca_3(PO_4)_2$ and $6Ca_2SiO_4{\cdot}Ca_3(PO_4)_2$, in the slag without Na_2O. When Na_2O is added to the dephosphorization slag, some Na will replace the Ca in the phosphorus-containing phase, thus forming a $Ca_2SiO_4{\cdot}Ca_2Na_2(PO_4)_2$ phase and some Na_3PO_4 phase. Chuanming Du [27] and Kan Yu [28] also found that alkaline oxides, such as Na_2O, are conducive to the formation of a phosphorus-rich solid solution in dephosphorization slag. In addition, Figure 2 shows that the addition of Na_2O will also form a low-melting-point phase, such as $Na_2Si_2O_5$, which can achieve rapid slag melting in the early stage of converter smelting and promote dephosphorization reactions.

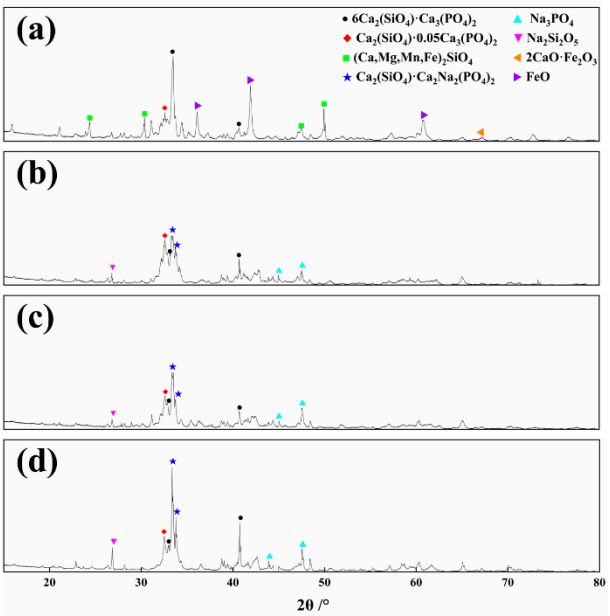


Figure 2. XRD results of dephosphorization slag. (**a**) No. 1 slag sample; (**b**) No. 2 slag sample; (**c**) No. 3 slag sample; (**d**) No. 4 slag sample.

Figure 3 shows the SEM observation results of the experiment's dephosphorization slag samples. The figure indicates that the dephosphorization slag mainly has a white area and a gray area, which is consistent with the research results of previous researchers [29–31]; however, they all found that the gray area can be divided into a gray phosphorus-containing

area and a gray phosphorus-free area. In this regard, the energy spectrum analyzer was used to quantitatively analyze the components in different positions of the white and gray areas; the results are shown in Table 5. They indicate that there are more elements of Fe, Mg, Mn, and O in the white area 1, which is an iron-rich phase; the gray area 2 is rich in phosphorus, and its P element is greater than the other areas; and the gray area 3 is the matrix phase, with mainly the elements Ca, Si, and O.

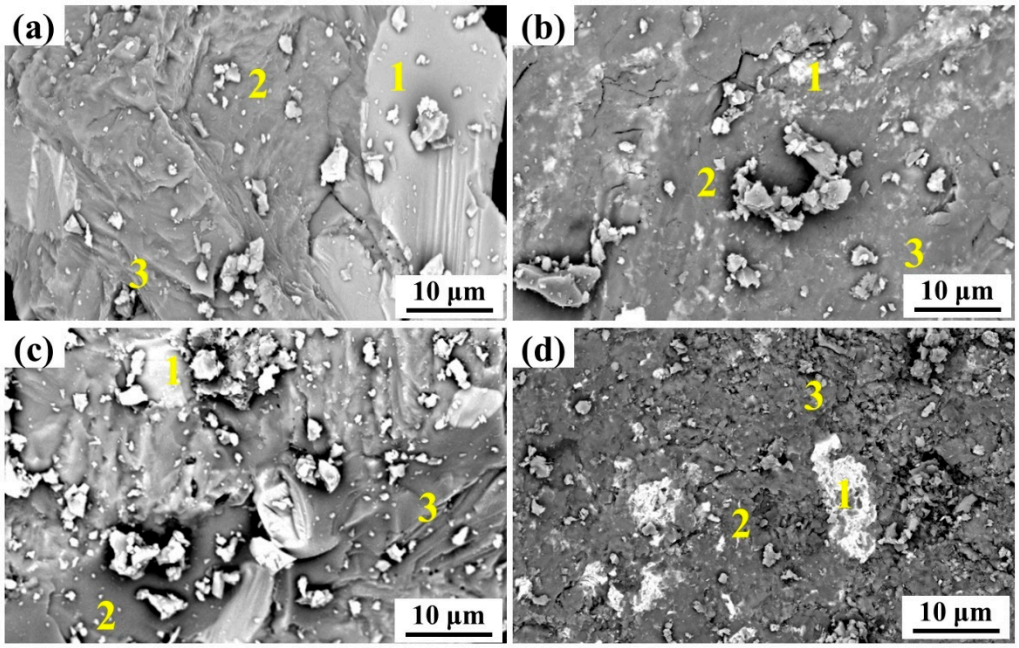


Figure 3. SEM results of dephosphorization slag sample. (**a**) No. 1 slag sample; (**b**) No. 2 slag sample; (**c**) No. 3 slag sample; (**d**) No. 4 slag sample. 1 iron-rich phase; 2 phosphorus-rich phase; 3 matrix phase.

Table 5. Energy spectrum analysis results of dephosphorization slag (mass fraction, %).

Heats	Areas	Ca	Si	O	Mg	Fe	P	Mn	Na
No. 1	1	0.71	0.28	27.79	15.38	45.23	0	10.61	0
	2	38.50	13.57	38.02	4.97	2.94	0.93	1.06	0
	3	42.47	17.61	29.38	5.32	3.98	0.04	1.20	0
No. 2	1	3.72	0.38	16.49	23.23	46.89	0	9.20	0.09
	2	45.06	15.75	32.25	2.32	1.18	1.15	1.43	1.01
	3	35.57	16.34	36.33	5.77	4.17	0.08	1.57	0.17
No. 3	1	3.39	1.58	14.37	11.81	51.17	0	17.20	0.48
	2	39.23	13.78	36.26	0.95	4.98	1.95	1.11	1.75
	3	36.73	17.57	37.22	2.57	3.57	0.07	1.95	0.32
No. 4	1	3.30	1.21	28.23	9.97	46.05	0	10.91	0.33
	2	36.62	16.66	35.20	2.56	2.19	2.15	1.88	2.75
	3	36.51	20.24	30.79	4.37	5.74	0.12	1.64	0.59

Figures 4 and 5 show the element mapping analysis results of the No. 1 slag sample and the No. 3 slag sample, respectively. The distribution of each element in Figure 4 indicates that Ca, Si, O, and P are distributed in the gray area 2, which is consistent with the energy spectrum analysis results in Table 5. Combined with the XRD phase analysis results in Figure 2, these elements exist in the form of a phosphate phase. The distribution map of each element in Figure 5 indicates that after adding Na_2O to the dephosphorization slag, the Na element mainly exists in the gray area containing phosphorus. Combined with the XRD analysis in Figure 2, it mainly forms a $Ca_2SiO_4 \cdot Ca_2Na_2(PO_4)_2$ phase.

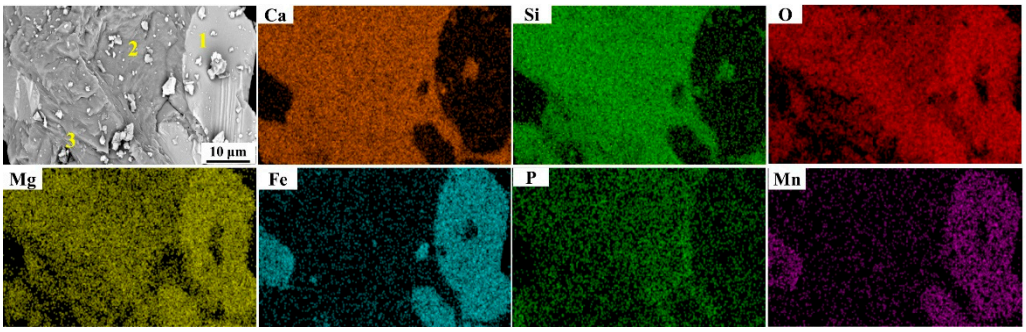


Figure 4. Element mapping analysis result of No. 1 dephosphorization slag. 1 iron-rich phase; 2 phosphorus-rich phase; 3 matrix phase.

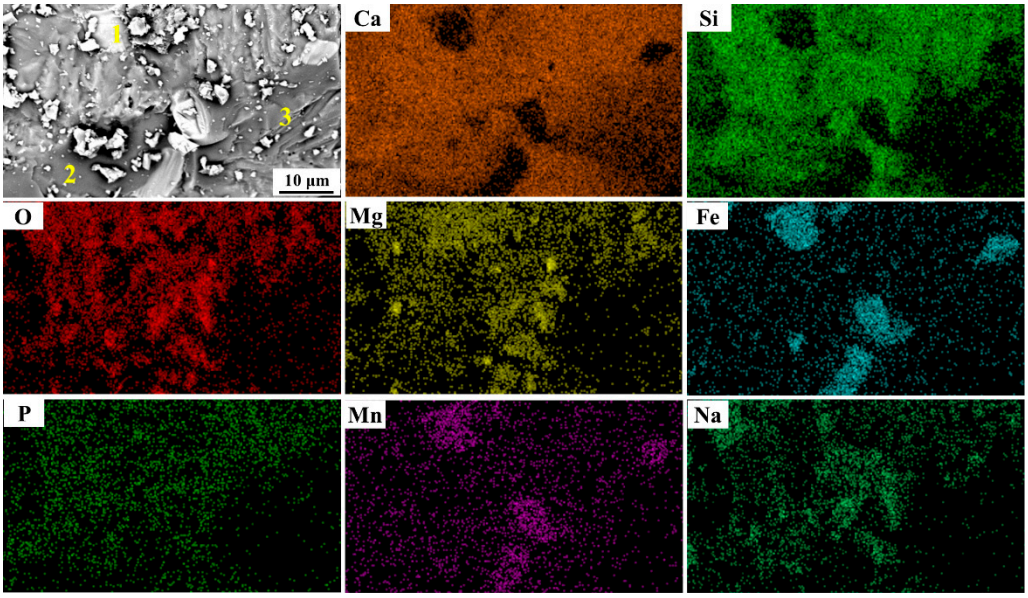


Figure 5. Element mapping analysis result of No. 3 dephosphorization slag. 1 iron-rich phase; 2 phosphorus-rich phase; 3 matrix phase.

3.2. Industrial Results

The phosphorus mass fraction and dephosphorization rate of the conventional heats and test heats after blowing 6 min and the end point are shown in Table 6. The composition of the molten iron used in the two production processes is the same. Table 6 shows that the average dephosphorization rate of the molten iron in the conventional heats blowing for 6 min is only 42.77%, while the test heats can reach 62.39%, and the dephosphorization rate in the early stage of the converter increased by 19.62%. In addition, the average phosphorus mass fraction of the molten iron in the test heats is 0.041%, which is 0.019% lower than that in the conventional heats.

Table 6. Average value of phosphorus mass fraction and dephosphorization rate.

Heats	P Mass Fraction/%		Dephosphorization Rate/%	
	6 min	End Point	6 min	End Point
Conventional	0.060	0.040	42.77	62.14
Test	0.041	0.030	62.39	72.03

Moreover, the average dephosphorization rate at the end of the conventional heats is 62.14%, and the average dephosphorization rate at the end of the test heats can reach 72.03%, which is a 9.89% increase. When $w(Na_2O)$ reached 0.79% in the dephosphorization

slag designed by Zhiqiang Zhou [20], the dephosphorization rate increased about 10%. In addition, the average mass fraction of the phosphorus at the end of the test heats is 0.03%, which is 0.01% lower than that of the conventional heats.

The average value of the final slag compositions of the conventional and test heats is shown in Table 7. The average basicity of the final slag of the test heats is 2.31, which is 0.19% lower than that of the conventional heats. The average $w(P_2O_5)$ in the final slag of the test heats is 2.83%, which is 0.36% higher than the conventional heats. The dephosphorization effect is enhanced, while reducing the consumption of materials such as lime. In addition, the average value of T.Fe in the final slag of the test heats is 14.93%, which is 0.69% lower than 15.62% of the conventional heats.

Table 7. Comparison of converter slag compositions (mass fraction, %).

Heats	CaO	T.Fe	MgO	MnO	SiO_2	Al_2O_3	P_2O_5	Na_2O	R
Conventional	43.81	15.62	9.60	5.04	17.54	2.79	2.47	<0.01	2.50
Test	41.69	14.93	9.55	5.38	18.00	2.82	2.83	0.16	2.31

The average value of the slagging materials consumption of the conventional and test heats is shown in Table 8. The table indicates that the average lime consumption of the test heats is 26.15 kg/t, which is 6.16 kg/t lower than that of the conventional heats. The change of the magnesium oxide ball consumption is not obvious; the average consumption of dolomite decreased by 2.67 kg/t; and the consumption of sodium-containing slagging material increased by 1.54 kg/t. The average consumption of slagging materials is 35.93 kg/t, which is 7.24 kg/t lower than that of the conventional heats. In addition, the average consumption of the iron and steel material in the test heats is 1052.23 kg/t, which is 1.37 kg/t lower than that in the conventional heats.

Table 8. Comparison of average material consumption ($kg \cdot t^{-1}$).

Heats	Lime	Magnesium Oxide Ball	Dolomite	Sodium-Containing Slag	Total Slag Consumption	Iron and Steel Consumption
Conventional	32.31	8.19	2.67	—	43.17	1053.60
Test	26.15	8.24	—	1.54	35.93	1052.23

4. Analysis and Discussion

4.1. Effect of Na_2O on Dephosphorization Reaction

In the conventional production process of the converter, the oxidative dephosphorization reaction occurs at the steel–slag interface. The relationship between the standard Gibbs free energy and the temperature of the dephosphorization reaction equations between CaO/Na_2O and molten iron [32–35] are shown in Figure 6. The figure shows that the Gibbs free energy of Equation (3) is lower than the other two reactions at the same temperature, which indicates that the dephosphorization reaction between Na_2O and molten iron occurs more easily.

4.2. Effect of Na_2O on Phosphorus Distribution Ratio

4.2.1. Establishment of Phosphorus Distribution Ratio Model

The phosphorus distribution ratio (L_P) is one of the important parameters reflecting the dephosphorization ability of slag. As the phase diagram can accurately reflect the structure and thermodynamic properties of metallurgical melts, many scholars [36–41] used Ion and Molecule Coexistence Theory (IMCT) to characterize the physical and chemical properties of slag, and then obtained an IMCT-L_P prediction model with high accuracy. Based on IMCT, a calculation model of the phosphorus distribution ratio of slag containing Na_2O was established in this article, and the influence of Na_2O on the phosphorus distribution ratio between slag and molten iron was discussed.

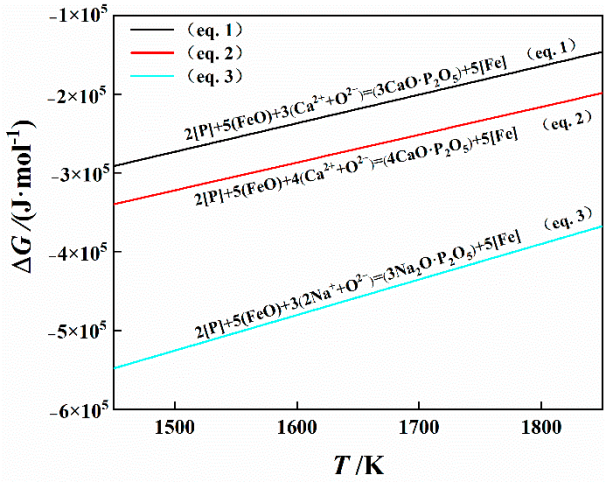


Figure 6. Relationship between standard Gibbs free energy and temperature of reaction equations.

Combined with the phase diagram, we determined that the slag has the following structural units, in which the chemical reaction formula, standard Gibbs free energy, and equilibrium constant of complex molecules can be referred to [32–35].

(1) Ions: Ca^{2+}, Fe^{2+}, O^{2-}, Mn^{2+}, Mg^{2+}, Na^{+};
(2) Simple molecules: SiO_2, Al_2O_3, P_2O_5;
(3) Complex molecule: $CaO{\cdot}SiO_2$, $2CaO{\cdot}SiO_2$, $3CaO{\cdot}SiO_2$, $3CaO{\cdot}2SiO_2$, $MgO{\cdot}SiO_2$, $2MgO{\cdot}SiO_2$, $CaO{\cdot}Al_2O_3$, $CaO{\cdot}2Al_2O_3$, $CaO{\cdot}6Al_2O_3$, $3CaO{\cdot}Al_2O_3$, $12CaO{\cdot}7Al_2O_3$, $3Al_2O_3{\cdot}2SiO_2$, $2FeO{\cdot}SiO_2$, $MnO{\cdot}SiO_2$, $2MnO{\cdot}SiO_2$, $Na_2O{\cdot}Al_2O_3$, $FeO{\cdot}Al_2O_3$, $MnO{\cdot}Al_2O_3$, $MgO{\cdot}Al_2O_3$, $2CaO{\cdot}P_2O_5$, $3CaO{\cdot}P_2O_5$, $4CaO{\cdot}P_2O_5$, $3FeO{\cdot}P_2O_5$, $4FeO{\cdot}P_2O_5$, $3MnO{\cdot}P_2O_5$, $2MgO{\cdot}P_2O_5$, $3MgO{\cdot}P_2O_5$, $3Na_2O{\cdot}P_2O_5$, $CaO{\cdot}MgO{\cdot}SiO_2$, $CaO{\cdot}MgO{\cdot}2SiO_2$, $2CaO{\cdot}MgO{\cdot}2SiO_2$, $3CaO{\cdot}MgO{\cdot}2SiO_2$, $CaO{\cdot}Al_2O_3{\cdot}2SiO_2$, $2CaO{\cdot}Al_2O_3{\cdot}SiO_2$, $Na_2O{\cdot}Al_2O_3{\cdot}2SiO_2$, $Na_2O{\cdot}Al_2O_3{\cdot}6SiO_2$.

The total equilibrium mole number of all the structural units in 100 g slag can be calculated by the following formula:

$$\sum n_i = 2n_1 + n_2 + 2n_3 + \ldots + n_{c1} + \ldots + n_{c36} \quad (1)$$

where n_1~n_6 represents the molar number of simple components under equilibrium conditions; n_{c1}~n_{c36} represents the molar number in the equilibrium of 36 composite molecules; and $\sum n_i$ represents the sum of the molar numbers of each structural unit in the slag during equilibrium, mol.

N_i is defined as the mass action concentration of the structural unit *i*, which is equal to the ratio of the equilibrium molar number of structural unit *i* to the total molar number of all structural units in the equilibrium system. The expression is as follows:

$$N_i = \frac{n_i}{\sum n_i} \quad (2)$$

We assume that the mole fractions of the initial oxides before the equilibrium of 100 g slag are $b_1 = n^0_{CaO}$, $b_2 = n^0_{SiO_2}$, $b_3 = n^0_{FeO}$, $b_4 = n^0_{MnO}$, $b_5 = n^0_{MgO}$, $b_6 = n^0_{Al_2O_3}$, $b_7 = n^0_{Na_2O}$, $b_8 = n^0_{P_2O_5}$.

According to the law of the conservation of mass, the molar number of each oxide is constant before and after the reaction, and the conservation formulas can be established. Taking CaO as an example:

$$b_1 = (0.5N_1 + K_{c1}N_1N_2 + 2K_{c2}N_1^2N_2 + 3K_{c3}N_1^3N_2 + 3K_{c4}N_1^3N_2^2 + K_{c7}N_1N_6 + K_{c8}N_1N_6^2 + K_{c9}N_1N_6^6 + 3K_{c10}N_1^3N_6 + 12K_{c11}N_1^{12}N_6^7 + 2K_{c20}N_1^2N_8 + 3K_{c21}N_1^3N_8 + 4K_{c22}N_1^4N_8 + K_{c29}N_1N_2N_5 + K_{c30}N_1N_2^2N_5 + 2K_{c31}N_1^2N_2^2N_5 + 3K_{c32}N_1^3N_2^2N_5 + K_{c33}N_1N_2^2N_6 + 2K_{c34}N_1^2N_2N_6)\sum n_i \quad (3)$$

When the slag is balanced, the sum of the mole fractions of all structural units is 1, and the following formula can be obtained:

$$N_1 + N_2 + \ldots + N_8 + N_{c1} + \ldots + N_{c36} = N_1 + N_2 + \ldots + N_8 + K_{c1}N_1N_2 + \ldots + K_{c36}N_2^6N_6N_7 = 1 \quad (4)$$

Calculated by MATLAB software, the values of N_1~N_8 and $\sum n_i$ can be determined.

There are 10 dephosphorization products in the slag. The chemical reactions, standard Gibbs free energy, and equilibrium constant [32–35] are shown in Table 9, $a_{[P]} = [\%P]f_P$.

Table 9. Standard Gibbs free energy and equilibrium constant of dephosphorization reaction.

Dephosphorization Reactions	$\Delta_r G_m^\theta$/J·mol^{-1}	K_{ci}^θ
2[P] + 5(FeO) = (P_2O_5) + 5[Fe]	−122,412 + 312.522 T	$K_8 = \frac{N_8 a_{[Fe]}^5}{N_3^5 a_{[P]}^2}$
2[P] + 5(FeO) + 2(Ca^{2+} + O^{2-}) = (2CaO·P_2O_5) + 5[Fe]	−606,784 + 285.953 T	$K_{c20} = \frac{N_{c20} a_{[Fe]}^5}{N_1^2 N_3^5 a_{[P]}^2}$
2[P] + 5(FeO) + 3(Ca^{2+} + O^{2-}) = (3CaO·P_2O_5) + 5[Fe]	−816,975.125 + 362.419 T	$K_{c21} = \frac{N_{c21} a_{[Fe]}^5}{N_1^3 N_3^5 a_{[P]}^2}$
2[P] + 5(FeO) + 4(Ca^{2+} + O^{2-}) = (4CaO·P_2O_5) + 5[Fe]	−851,492.98 + 352.822 T	$K_{c22} = \frac{N_{c22} a_{[Fe]}^5}{N_1^4 N_3^5 a_{[P]}^2}$
2[P] + 5(FeO) + 3(Fe^{2+} + O^{2-}) = (3FeO·P_2O_5) + 5[Fe]	−552,816 + 405.23 T	$K_{c23} = \frac{N_{c23} a_{[Fe]}^5}{N_3^3 N_3^5 a_{[P]}^2}$
2[P] + 5(FeO) + 4(Fe^{2+} + O^{2-}) = (4FeO·P_2O_5) + 5[Fe]	−504,243 + 359.889 T	$K_{c24} = \frac{N_{c24} a_{[Fe]}^5}{N_3^4 N_3^5 a_{[P]}^2}$
2[P] + 5(FeO) + 3(Mn^{2+} + O^{2-}) = (3MnO·P_2O_5) + 5[Fe]	−648,833.411 + 414.571 T	$K_{c25} = \frac{N_{c25} a_{[Fe]}^5}{N_4^3 N_3^5 a_{[P]}^2}$
2[P] + 5(FeO) + 2(Mg^{2+} + O^{2-}) = (2MgO·P_2O_5) + 5[Fe]	45,957 − 26.835 T	$K_{c26} = \frac{N_{c26} a_{[Fe]}^5}{N_5^2 N_3^5 a_{[P]}^2}$
2[P] + 5(FeO) + 3(Mg^{2+} + O^{2-}) = (3MgO·P_2O_5) + 5[Fe]	−609,127.5 + 349.366 T	$K_{c27} = \frac{N_{c27} a_{[Fe]}^5}{N_5^3 N_3^5 a_{[P]}^2}$
2[P] + 5(FeO) + 3(2Na^{2+} + O^{2-}) = (3Na_2O·P_2O_5) + 5[Fe]	−1,202,452 + 451.222 T	$K_{c28} = \frac{N_{c28} a_{[Fe]}^5}{N_7^2 N_3^5 a_{[P]}^2}$

According to Henry's law, when [%P] approaches 0, f_P approaches 1. The calculation formula for the phosphorus distribution ratio between slag and molten iron can be obtained:

$$L_P = \frac{(\%P_2O_5)}{[\%P]^2} = M_{P_2O_5} N_3^5 f_P^2 (K_8 + K_{c20}N_1^2 + K_{c21}N_1^3 + K_{c22}N_1^4 + K_{c23}N_3^3 + K_{c24}N_3^4 + K_{c25}N_4^3 + K_{c26}N_5^2 + K_{c27}N_5^3 + K_{c28}N_7^3)\sum n_i \quad (5)$$

In order to further verify the applicability and accuracy of the model, this paper refers to the measured data of the dephosphorization experiment in the relevant literature [17,42,43] and compares them with the model calculation results, as shown in Figure 7. The figure shows that the L_P calculated by the model is close to the L_P measured by the experiment, indicating that the calculation results of this model are highly reliable.

4.2.2. Effect of Na_2O on Phosphorus Distribution Ratio

The effects of $w(Na_2O)$ on L_P at 1573 K, 1623 K, and 1673 K are shown in Figure 8. The figure indicates that a small amount of Na_2O can significantly improve the phosphorus distribution ratio. Free oxygen ions can promote the formation of phosphate, according to the IMCT, and the free oxygen ions in the slag are generated by the dissociation of alkaline oxides [33]. As an alkali metal element, sodium is more alkaline than CaO, and it is easier to dissociate free oxygen ions, thus it shows better dephosphorization ability. In this industrial test, using the thermodynamic conditions of dephosphorization at lower

temperature in the early stage increased the $w(Na_2O)$ in slag to 0.5%, thereby ensuring the high phosphorus distribution ratio between the molten iron and slag and achieving the purpose of rapid dephosphorization in the early stage.

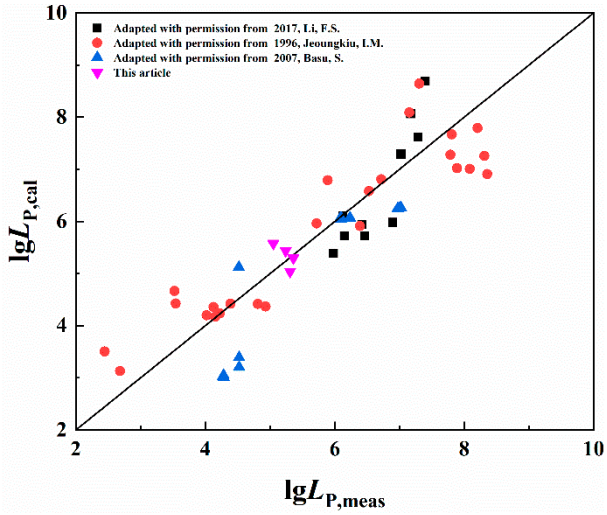


Figure 7. Comparison of calculated $\lg L_{P,cal}$ and measured $\lg L_{P,meas}$ [17,42,43].

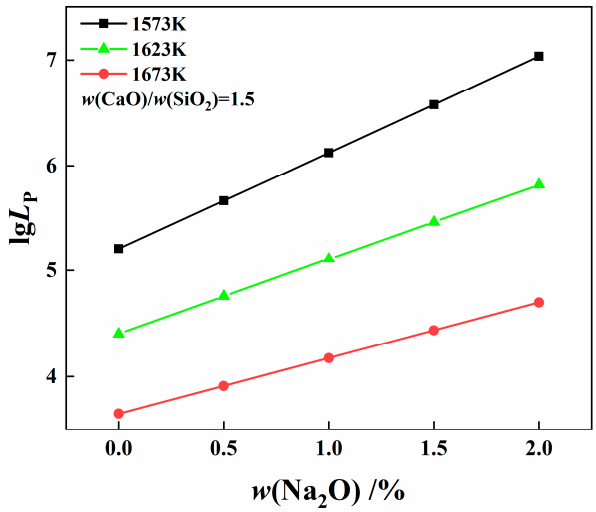


Figure 8. Effect of different mass fraction of Na_2O on $\lg L_P$.

According to the literature [44], Na_2CO_3 can be used as an additive in lime-based dephosphorization flux. Na_2CO_3 is decomposed into Na_2O and CO_2 by heating, and Na_2O can improve the phosphorus distribution ratio. However, Na_2O is highly active in the alkaline slag, which is easy to volatilize from the slag, and volatile Na_2O will cause serious corrosion to the furnace lining; therefore, the mass fraction of Na_2O in slag should not be too high. Thus, the $w(Na_2O)$ in the slag was controlled less than 1.0% in these industrial trial heats.

4.3. Effect of Na_2O on Physicochemical and Chemical Properties of Slag System

4.3.1. Effect of Na_2O on Melting Point of Slag

Figure 9 shows the liquid region of the CaO-FeO-SiO_2 slag system at 1573 K after adding the Na_2O calculated by FactSage8.1. It indicates that with the increasing of the $w(Na_2O)$ in the slag, the area of the liquid phase increases continuously, and the liquid phase region moves to the low w(FeO) region. Na_2O has a great influence on the liquidus in the region of low binary basicity and has little influence in the region of high binary

basicity. Figure 10 shows the experiment results of different fractions of Na_2O on the melting point of the tested slag. It indicates that with the increasing of the $w(Na_2O)$ in slag, the melting point decreases continuously. When the $w(Na_2O)$ increases from 0 to 0.5%, the melting point of the tested slag decreases from 1645 K to 1639 K, which is consistent with the law measured by Jiang Diao [11]. The addition of Na_2O can generate low-melting-point compounds, such as $Na_2Si_2O_5$ and $Na_2Ca_2Si_3O_9$, in the slag, which helps to reduce the melting point of the slag [45,46], achieve rapid slag melting in the early stage of converter smelting, and promote the dephosphorization reactions.

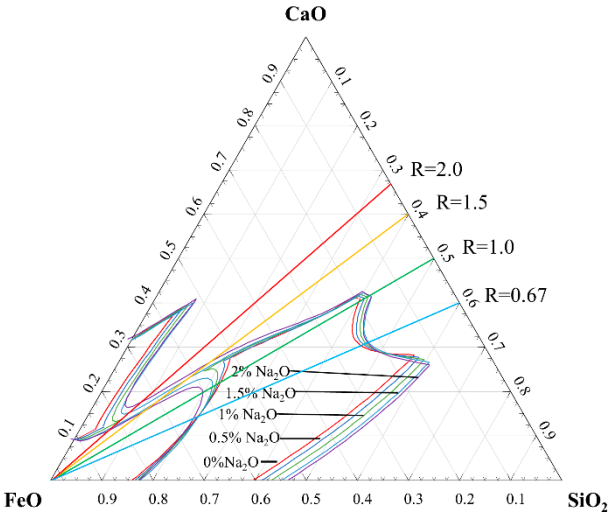


Figure 9. Liquid region of CaO-FeO-SiO_2 slag at 1573 K.

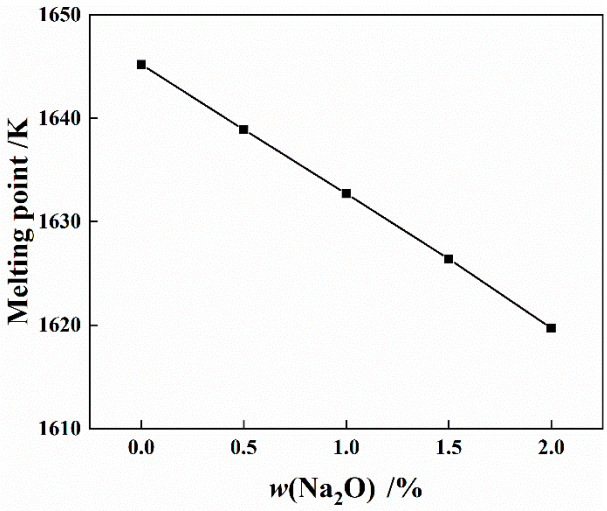


Figure 10. Effect of different mass fractions of Na_2O on melting point of slag system.

4.3.2. Effect of Na_2O on Viscosity of Slag

Figure 11 shows the viscosity change of the CaO-FeO-SiO_2 slag after adding the Na_2O calculated by FactSage8.1. It indicates that the viscosity of the slag decreases with the increasing of $w(Na_2O)$. After the viscosity of the slag is reduced, the fluidity is enhanced, the mass transfer capacity between the molten iron and slag is enhanced, and the dephosphorization reaction is promoted [47–49].

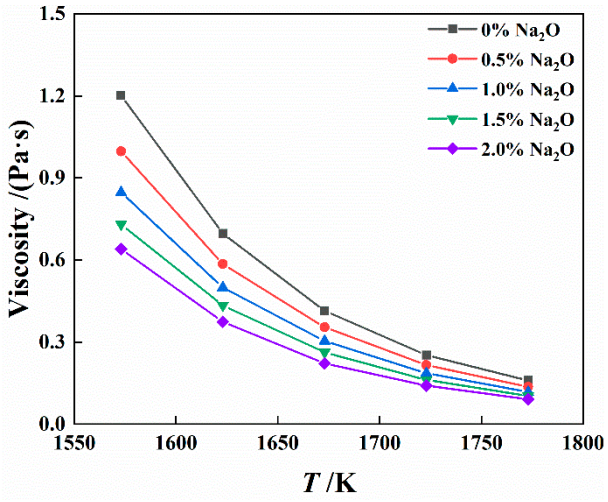


Figure 11. Effect of $w(Na_2O)$ on viscosity of CaO-25%FeO-SiO_2 slag (R = 1.5).

5. Conclusions

(1) With the increase of $w(Na_2O)$, the dephosphorization rate increases, and the Ca, Si, O, and P elements in the dephosphorization slag are distributed in the same area, mainly in the form of phosphate minerals, such as $Ca_2SiO_4 \cdot 0.05Ca_3(PO_4)_2$ and $6Ca_2SiO_4 \cdot Ca_3(PO_4)_2$. After adding Na_2O, part of the Na will replace the Ca in the phosphorus-containing phase, forming a $Ca_2SiO_4 \cdot Ca_2Na_2(PO_4)_2$ phase.

(2) After adding sodium-containing slagging material, the average dephosphorization rate of blowing for 6 min and at the end point can reach 62.39% and 72.03%, which are 19.62% and 9.89% higher, respectively, than the corresponding values of the conventional heats. The average final slag basicity of the test heats is 0.19% lower than that of the conventional heats, while the average $w(P_2O_5)$ of the final slag increases by 0.36%, and the average T.Fe decreases by 0.69%. The average slagging materials consumption of the test heats is 35.93 kg/t, which is 7.24 kg/t lower than that of the conventional heats.

(3) Through thermodynamic calculation, we found that with the increase of $w(Na_2O)$, the phosphorus distribution ratio between the slag and the molten iron increases significantly, the area of the liquid phase zone of the slag system increases continuously, and the viscosity decreases continuously.

Author Contributions: Investigation, B.G. and Y.Y.; Conceptualization, B.G.; methodology, Z.J.; formal analysis, D.Z. and B.G.; Data collection, B.G. and Y.Y.; Writing—original draft, B.G.; Writing—review and editing, D.Z.; Resources, Z.J.; Supervision, D.Z. All authors have read and agreed to the published version of the manuscript.

Funding: The authors are grateful for the support from the Open Competition Scientific and Technological Research Projects of Heilongjiang Province (2022ZXJ03A02) and the Jiangxi Provincial Technical Innovation Guidance Program (20202BDH80002).

Institutional Review Board Statement: Not applicable.

Informed Consent Statement: Not applicable.

Data Availability Statement: Not applicable.

Conflicts of Interest: The authors declare no conflict of interest.

References

1. Messier, R.W.; Li, L. Separating effects of phosphorus and sulfur in weld cracking of austenitic stainless steels for technological and economic benefits. *J. Adv. Mater.* **2001**, *33*, 3–13.
2. Ogawa, Y.; Yano, M.; Kitamura, S.; Hirata, H. Development of the continuous dephosphorization and decarburization process using BOF. *Tetsu-Hagané* **2001**, *87*, 21–28. [CrossRef] [PubMed]

3. Wang, X.H.; Zhu, G.S.; Li, H.B.; Lv, Y.C. Investigation on "slag remaining + double-slag" BOF steelmaking technology. *Chin. Metall.* **2013**, *23*, 40–46.
4. Gao, S.Y.; Tian, Z.H.; Zhu, L.X.; Zhao, C.L.; Yan, Z.H.; Luo, B.G.; Wei, G. Study on the dephosphorization of hot metal in converter. *Chin. J. Eng.* **2011**, *33*, 63–67.
5. Kang, F.; Lu, Z.X.; Jiang, X.F.; Zhong, Z.M. Research and development of BRP technology at Baosteel. *Steel* **2005**, *3*, 25–28.
6. Zhou, C.G.; Hu, J.Z.; Ai, L.Q.; Wang, S.H.; Yang, H.Z.; Chen, H. Research progress and prospect of dephosphorization in steelmaking converter. *J. Iron Steel Res.* **2021**, *33*, 183–195.
7. Liu, J.; Li, G.Q.; Zhu, C.Y.; Wang, C.A. Research progress in treatment of high phosphorus iron ore and dephosphorization of high phosphorus hot metal. *J. Mater. Metall.* **2007**, *23*, 173–179.
8. Pak, J.J.; Fruehan, R.J. The effect of Na_2O on dephosphorization by CaO-based steelmaking slags. *Metall. Trans. B* **1991**, *22*, 39–46. [CrossRef]
9. Pak, J.J.; Fruehan, R.J. Soda slag system for hot metal dephosphorization. *Metall. Trans. B* **1986**, *17*, 797–804. [CrossRef]
10. Li, G.Q.; Hamano, T.; Tsukihashi, F. The effect of Na_2O and Al_2O_3 on dephosphorization of molten steel by high basicity MgO saturated CaO-FeO_x-SiO_2 slag. *ISIJ Int.* **2005**, *45*, 12–18. [CrossRef]
11. Diao, J. Effect of Al_2O_3 and Na_2O on dephosphorization of high phosphorus hot metal. *J. Iron Steel Res.* **2013**, *25*, 9–13.
12. Du, C.M.; Lv, N.N.; Su, C.; Liu, W.M.; Yang, J.X.; Wang, H.C. Distribution of P_2O_5 between solid solution and liquid phase in dephosphorization slag of CaO-SiO_2-FeO-P_2O_5-Na_2O system. *J. Iron Steel Res. Int.* **2019**, *26*, 1162–1170. [CrossRef]
13. Wrampelmeyer, J.C.; Dimitrov, S.; Janke, D. Dephosphorization equilibria between pure molten iron and CaO-saturated FeO_n-CaO-SiO_2 and FeO_n-CaO-Al_2O_3 slags. *Steel Res.* **1989**, *60*, 539. [CrossRef]
14. Xing, W.; Wu, L.; Li, S.Q.; Yao, L.; Liu, R.Z. Experimental study on the melting temperature characteristic of the CaO-FeO-Al_2O_3-SiO_2 slag system. *Chin. J. Eng.* **2014**, *36*, 603–607.
15. Zhang, H.Y.; Jiang, Z.H.; Wang, W.Z.; Liu, X.; Gu, W.B.; Wang, J. Effect of BaO and Na_2O on equilibrium phosphorus content in LF refining liquid steel. *Spec. Steel* **2002**, *1*, 14–16.
16. Taposhe, G.I.A.; Khajavi, L.T. Removal of phosphorus from Si-Fe alloy by CaO-Al_2O_3-SiO_2-Na_2O slag refining. *J. Miner. Met. Mater. Soc.* **2021**, *73*, 729–735. [CrossRef]
17. Li, F.S.; Li, X.P.; Yang, S.F.; Zhang, Y.L. Distribution ratios of phosphorus between CaO-FeO-SiO_2-Al_2O_3/Na_2O/TiO_2 slags and carbon-saturated iron. *Metall. Mater. Trans. B* **2017**, *48*, 2367–2378. [CrossRef]
18. Li, F.S.; Li, X.P.; Zhang, Y.L.; Gao, M. Phosphate capacities of CaO-FeO-SiO_2-Al_2O_3/Na_2O/TiO_2 slags. *High Temp. Mater. Process.* **2019**, *38*, 50–59. [CrossRef]
19. Li, X.P.; Gao, J.T.; Zhang, Y.L.; Xing, L.L.; Zou, L. Distribution behavior of phosphorus between CaO-FeO-SiO_2-Al_2O_3/Na_2O/TiO_2 slags and carbon-saturated iron. *Steel* **2017**, *52*, 18–23. [CrossRef]
20. Zhou, Z.Q.; Zhu, Z.Z.; Ding, Y.C.; Zhou, S.N. Effect of Na_2O on dephosphorization for high phosphorus Si-Mn alloys. *Steel* **2017**, *52*, 13–17.
21. Xuan, X.Y.; Shi, Z.; Qi, X.; Cai, J.W. Study on dephosphorization of high-phosphorus hot metal in CaO-SiO_2-FeO-Na_2O-Al_2O_3 slag system. *Min. Metall.* **2015**, *24*, 51–54.
22. Moriya, T.; Fujii, M. Dephosphorization and desulfurization of molten pig iron by Na_2CO_3. *Trans. Iron Steel Inst. Jpn.* **1981**, *21*, 732–741. [CrossRef]
23. Maddocks, W.R.; Turkdogan, E.T. The effect of sodium oxide additions to steelmaking slags dephosphorization of steel by soda-slags. *J. Iron Steel Inst.* **1952**, *171*, 128–136.
24. Oelsen, W. The dephosphorization and desulfurization of high-carbon iron melts with the production of water-soluble high phosphorus slags. *Arch Eisenhuttenw* **1965**, *36*, 861–871.
25. Ito, K.; Sang, N. Phosphorus distribution between basic slags and carbon-saturated iron at hot-metal temperatures. *Trans. Iron Steel Inst. Jpn.* **1985**, *25*, 355–362. [CrossRef]
26. Marukawa, K.; Shirota, Y.; Anezaki, S.; Hirahara, H. Refining process of molten iron by sodium carbonate. *Tetsu-Hagané* **1981**, *67*, 323. [CrossRef]
27. Du, C.M.; Gao, X.; Ueda, S.; Kitamura, S.Y. Effect of Na_2O addition on phosphorus dissolution from steelmaking slag with high P_2O_5 content. *J. Sustain. Metall.* **2017**, *3*, 671–682. [CrossRef]
28. Yu, K.; Zhang, Y.L.; Li, F.S.; Gao, M. Effect of Al_2O_3/TiO_2/Na_2O on enrichment of phosphorus in P-bearing steelmaking slag. *J. Iron Steel Res. Int.* **2019**, *26*, 796–805. [CrossRef]
29. Wang, D.Z.; Bao, Y.P.; Wang, M. Study on the enrichment behavior of phosphorus in high phosphorus converter slag. *Chin. J. Eng.* **2018**, *40*, 65–72.
30. He, S.; Liu, Y.Q.; Lin, L.; Hou, Z.X.; Huang, F.; Hu, Y.B. Effect of Na_2O on the enrichment behavior of phosphorus in the slag system CaO-SiO_2-Fe_2O_3-P2O_5. *Iron Steel Vanadium Titan.* **2022**, *43*, 140–145.
31. Lin, L.; Bao, Y.P.; Jiang, W.; Wu, Q.F. Effect of Na_2O on phosphorus enrichment and separation in P-bearing steelmaking slag. *ISIJ Int.* **2015**, *55*, 552–558. [CrossRef]
32. Zhang, J. *Computational Thermodynamics of Metallurgical Melts and Solutions*; Metallurgical Industry Press: Beijing, China, 2007.
33. Zhang, K.H.; Zhang, Y.L.; Li, F.S.; Wu, T. A thermodynamic model for calculation of sulfur distribution ratio between CaO-SiO_2-Al_2O_3-Na_2O-TiO_2-(MgO) slag and carbon saturated hot metal. *J. Iron Steel Res.* **2018**, *30*, 265–272.

34. Sun, J.L.; Liu, C.J.; Jiang, M.F. Thermodynamic model of dephosphorization of CaO-SiO_2-FeO-Al_2O_3-Na_2O-TiO_2-P_2O_5 slag system. *Iron Steel Vanadium Titan.* **2021**, *42*, 146–151+178.
35. Gong, W.; Jiang, Z.H.; Zhan, D.P. Intelligent information technology application association: The model of mass action concentration for slag system of CaO-SiO_2-$A1_2O_3$-MgO and its application. In Proceedings of the 2011 AASRI Conference on Artificial Intelligence and Industry Application (AASRI-AIIA 2011 V4), Male, Maldives, 23–24 May 2011; American Applied Sciences Research Institute: Miramar, FL, USA, 2011; p. 4.
36. Yang, X.M.; Duan, J.P.; Shi, C.B.; Zhang, M.; Zhang, Y.L.; Wang, J.C. A thermodynamic model of phosphorus distribution ratio between CaO-SiO_2-MgO-FeO-Fe_2O_3-MnO-Al_2O_3-P_2O_5 slags and molten steel during a top-bottom combined blown converter steelmaking process based on the ion and molecule coexistence theory. *Metall. Mater. Trans. B* **2011**, *42*, 738–770. [CrossRef]
37. Li, P.C.; Zhang, J.L. Retraction: A prediction model of phosphorus distribution between CaO-SiO_2-MgO-FeO-Fe_2O_3-P_2O_5 slags and liquid iron. *ISIJ Int.* **2014**, *54*, 756–765. [CrossRef]
38. Zhang, J. Coexistence theory of slag structure and its application to calculation of oxidizing capability of slag melts. *J. Iron Steel Res. Int.* **2003**, *10*, 1–10.
39. Yang, X.M.; Li, J.Y.; Zhang, M.; Chai, G.M.; Zhang, J. Prediction model of sulfide capacity for CaO-FeO-Fe_2O_3-Al_2O_3-P_2O_5 slags in a large variation range of oxygen potential based on the ion and molecule coexistence theory. *Metall. Mater. Trans. B* **2014**, *45*, 2118–2137. [CrossRef]
40. Yang, X.M.; Li, J.Y.; Zhang, M.; Zhang, J. Prediction model of sulphur distribution ratio between CaO-FeO-Fe_2O_3-Al_2O_3-P_2O_5 slags and liquid iron over large variation range of oxygen potential during secondary refining process of molten steel based on ion and molecule coexistence theory. *Ironmak. Steelmak.* **2016**, *43*, 39–55. [CrossRef]
41. Sun, Y.H.; Zhao, C.L.; Luo, L.; Zhao, Z.C. Calculation and analysis of slag phosphate capacity and prediction model in 300 t top and bottom-blowing converter. *Chin. J. Eng.* **2016**, *38*, 83–89.
42. Jeoungkiu, I.M.; Morita, K.; Sano, N. Phosphorus distribution ratios between CaO-SiO_2-Fe_tO slags and carbon-saturated iron at 1573 K. *ISIJ Int.* **1996**, *36*, 517–521.
43. Basu, S.; Lahiri, A.K.; Seetharaman, S. Phosphorus partition between liquid steel and CaO-SiO_2-P_2O_5-MgO slag containing low FeO. *Metall. Mater. Trans. B* **2007**, *38*, 357. [CrossRef]
44. Li, J.; Yue, K.X. Study on dephosphorizing flux containing CaO-Fe_2O_3-CaF_2-Al_2O_3-Na_2CO_3 for hot metal pretreatment. *J. Anhui Univ. Technol. (Nat. Sci. Ed.)* **2003**, *20*, 177–180.
45. Niekerk, W.H.V.; Dippenaar, R.J. Thermodynamic aspects of Na_2O and CaF_2 containing lime-based slags used for the desulphurization of hot-metal. *ISIJ Int.* **1993**, *33*, 59–65. [CrossRef]
46. Takahira, N.; Hanao, M.; Tsukaguchi, Y. Viscosity and solidification temperature of SiO_2-CaO-Na_2O melts for fluorine free mould flux. *ISIJ Int.* **2013**, *53*, 818–822. [CrossRef]
47. Sukenaga, S.; Saito, N.; Kawakami, K.; Nakashima, K. Viscosities of CaO-SiO_2-Al_2O_3-(R_2O or RO) melts. *ISIJ Int.* **2006**, *46*, 352–358. [CrossRef]
48. Chen, C.Y.; Jiang, Z.H.; Li, Y.; Sun, M.; Chen, K.; Wang, Q.; Li, H.B. Effect of Na_2O and Rb_2O on inclusion removal in C96V saw wire steels using low-basicity LF (Ladle Furnace) refining slags. *Metals* **2018**, *8*, 691. [CrossRef]
49. Kim, H.; Kim, W.H.; Park, J.H.; Min, D.J. A study on the effect of Na_2O on the viscosity for ironmaking slags. *Steel Res. Int.* **2010**, *81*, 17–24. [CrossRef]

Disclaimer/Publisher's Note: The statements, opinions and data contained in all publications are solely those of the individual author(s) and contributor(s) and not of MDPI and/or the editor(s). MDPI and/or the editor(s) disclaim responsibility for any injury to people or property resulting from any ideas, methods, instructions or products referred to in the content.